metals

MDPI

Article

Effect of Preheating Temperature on Microstructure and Properties of 42CrMo4/38MnVS6 Heterogeneous Laser Welded Joint

Jinlong Su, Xiaoming Qiu *, Fei Xing and Ye Ruan *

Key Laboratory of Automobile Materials Ministry of Education, School of Materials Science and Engineering, Jilin University, Changchun 130022, China

* Correspondence: qiuxm13@163.com (X.Q.); ruanye@jlu.edu.cn (Y.R.); Tel.: +86-139-4414-4493 (X.Q.); +86-131-5436-5903 (Y.R.)

Received: 23 July 2019; Accepted: 6 August 2019; Published: 8 August 2019

Abstract: Laser-welded forged steel pistons can meet the needs of the new era of heavy truck engines. 42CrMo4 and 38MnVS6 are widely used as piston materials due to the good mechanical properties. This study investigates the influence of preheating on microstructure and mechanical properties of 42CrMo4/38MnVS6 laser welding joint. The experimental results show preheating increases the laser absorption capacity of the metal, which can lead to an increase in weld width. The microstructure of weld is the high-hardness and poor toughness twin martensite without preheating. As the temperature of preheating increases, the twin martensite in the weld begins to transform into lath martensite and regenerates ferrite and bainite. As the preheating temperature increases, the plane fracture toughness (K1C) of the weld increases and then decreases, reaching the highest value of 2322.94 MPa·mm$^{-1/2}$ at 150 °C. Compared with no preheating conditions, the tensile strength of the welded joint after preheating is improved. The fracture mode of welded joints changes from brittle fracture to ductile fracture. When the preheating temperature is 100–200 °C, the tensile strength of the welded joint reaches 1018.1–1032.5 MPa; when the preheating temperature is 250 °C–300 °C, the tensile strength decreases.

Keywords: 42CrMo4; 38MnVS6; preheat; laser welding; microstructure; plane fracture toughness; tensile strength

1. Introduction

42CrMo4 is a type of medium carbon steel that provides high fatigue limit and good impact resistance. 38MnVS6 steel has high yield strength and good wear resistance. The heavy-duty diesel engine piston which adopts 42CrMo4 as the piston top and 38MnVS6 as the piston skirt can withstand high mechanical load and thermal load. It is beneficial to improve the combustion efficiency of the engine and reduce the fuel consumption [1–4]. The core problem of heavy truck diesel engine pistons is the jointing of 42CrMo4 with 38MnVS6. 42CrMo4 and 38MnVS6 are medium carbon steels with high carbon content, which means the weld will have high hardening tendency and high crack sensitivity. The connection of 42CrMo4 and 438MnVS6 has been considered by welding researchers [5–7]. There are two problems with the welding of medium carbon steel that need to be solved. First, the quenched and hardened microstructure of weld should be avoided during welding. Second, welded joints need to have high strength and toughness [8–11]. Yoo et al. studied the influence of welding parameters on the weld penetration, the aspect ratio of the weld and the initiation of defects in the weld for the case of the laser welding of S45C medium carbon steel, the relationship between effective heat input and weld penetration was obtained through a large number of tests, and it was determined that

the heat input is in the range of 275 J/mm$^{0.5}$·s$^{0.5}$ to 435 J/mm$^{0.5}$·s$^{0.5}$, and there was no defect in the weld [12]. Kuryntsev et al. studied the effect of heat treatment on laser welded joints of 0.349C-1Cr-1Si steel. The results showed that the laser welded joint had the characteristics of high hardness and low elongation. After heat treatment, the elongation and ductility of the welded joint are improved [13]. Laser welding has a high energy density, and the base metal is not easy to deform after welding. It can optimize the piston structure and is conducive to the full combustion of fuel. Therefore, the development of laser welding forged steel piston has become one of the development directions of piston structure [14–17]. Preheating before welding can increase the laser absorption rate of the metal and reduce the cooling rate of the weld, adjust the stress distribution of the welded joint, avoid the generation of hardened structure in the weld, and is one of the welding methods to effectively improve the mechanical properties of the welded joint [18,19].

At present, there are more studies on laser welding of aluminum alloy and low carbon steel with preheating, but less on medium carbon steel [20–22]. In this paper, the effect of preheating on the weld structure of 42CrMo4/38MnVS6 laser welding is studied, and the mechanical properties of welded joints under different preheating temperature are compared and analyzed, which provides the basis of experimental and theoretical for the application of laser welding technology in a forged steel piston.

2. Materials and Methods

2.1. Materials

The test materials were 42CrMo4 and 38MnVS6 with a size of 45 × 55 × 4 mm. The chemical composition is shown in Table 1 and the mechanical properties are shown in Table 2. 42CrMo4 and 38MnVS6 are medium carbon low alloy steel. 42CrMo4 steel belongs to the Cr–Mo steel system and has good strength and toughness. The Mo element can reduce the temper brittleness of steel and increase the high temperature strength. 38MnVS6 belongs to Mn–V steel system, V can improve the strength, plasticity and toughness of steel, and increase the high temperature tempering stability. According to the Equation (1) of the American Institute of Welding for carbon equivalent, the Ceq (carbon equivalent) of 42CrMo4 and 38MnVS6 are 0.79 and 0.63, respectively, the cold cracking tendency is high, and the weldability is poor.

$$Ceq = \omega\,(C) + \omega\,(Mn)/6 + \omega\,(Si)/24 + \omega\,(Ni)/15 + \omega\,(Cr)/5 + \omega\,(Mo)/4 + \omega\,(Cu)/13 + \omega\,(P)/2 \quad (1)$$

Table 1. Chemical composition of 42CrMo and 38MnVS6 (wt. %).

Material	C	Si	Mn	Cr	Mo	S	P	V	N	Fe
42CrMo4	0.41	0.32	0.62	1.02	0.23	0.04	0.035	-	-	base
38MnVS6	0.38	0.22	1.42	-	-	0.03	0.025	0.14	0.01	base

Table 2. Mechanical properties of 42CrMo and 38MnVS6.

Material	Tensile Strength (MPa)	Yield Strength (MPa)	Elongation (%)
42CrMo4	949	801	16.7
38MnVS6	895	698	15.2

2.2. Process Parameters of Laser Welding

HKW-1050 pulsed laser welding equipment manufactured by New Industry Photoelectric Technology Co., Ltd, Changchun, China. was used in the experiment. The laser used in the test was an Nd: YAG solid-state laser with a pulse welding method. The protective gas was argon at the purity of 99%, the gas was added as a cross jet and the flow rate was 15 L/min. The parameters of laser welding are shown in Table 3. The laser welding parameters were consistent under different preheating

conditions, ensuring that the samples were welded in keyhole model. The schematic diagram of the welding device is shown in Figure 1. Before welding, the base metal was treated by ultrasonic cleaning with acetone to remove surface dirt. During the welding experiment, the base metal was heated for 10 min at the predetermined heating temperature, and then laser welding was carried out. After the welding, the samples were cooled to room temperature together with the welding device.

Table 3. The parameters of laser welding.

Preheat (°C)	Pulse Current (A)	Pulse Width (ms)	Frequency
- 100 150 200 250 300	120	17.5	8

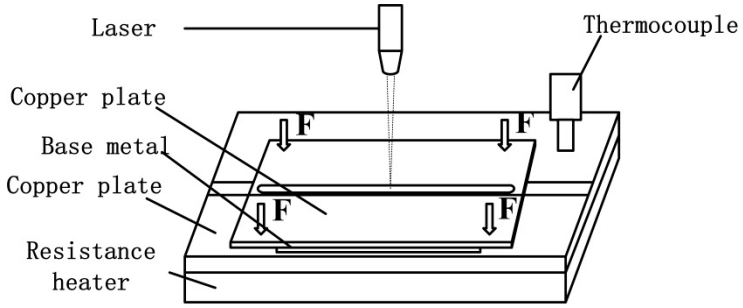

Figure 1. The schematic diagram of the welding device.

2.3. Metallography and XRD Test

The metallographic samples with the size of 10 × 20 × 4 mm were cut in a direction perpendicular to the weld by a wire cutter after 24 h after welding and sanded with 240#, 600#, 800#, 1000#, 1500# and 2000# sandpaper. The diamond polishing spray was used for polishing, and 4% nitric acid alcohol was used for corrosion. Microstructures of the joints were observed by Scope Axio ZEISS optical microscope and S-3400N scanning electron microscope. The phase of the sample was analyzed by D8 discover with GADDS X-ray diffractometer. The scanning range was 20°–90°, and the scanning speed was 1°/min.

2.4. Mechanical Performance Test

The microhardness of the weld was tested using an MH-3 microhardness tester. Five measurements were taken at different locations in the weld and the average was calculated. The plane toughness fracture test was carried out by INSTRON-1121 material testing machine with a loading force of 5 kN and a loading speed of 0.5 mm/min. Figure 2 is a schematic view showing the dimensions of the test specimen for plane fracture toughness. The test was carried out in accordance with ISO 15653:2018. The loading force is above the weld to ensure that the fracture occurs at the weld. The tensile test was carried out using an MIS8/0.22M electro-hydraulic servo tensile testing machine; the tensile speed was 1 mm/min. The size of tensile specimen is shown in Figure 3.

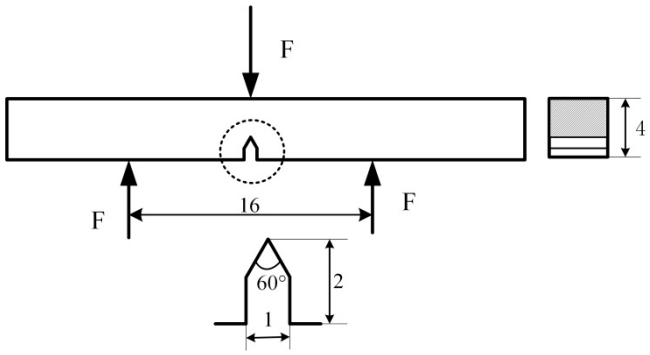

Figure 2. The sample size of plane fracture toughness test (mm).

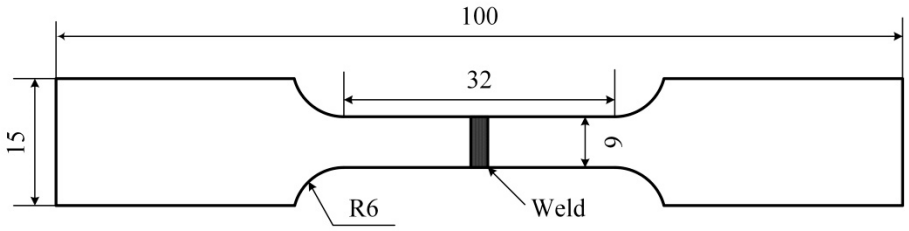

Figure 3. The sample size of tensile test (mm).

3. Results and Discussion

3.1. Effect of Preheating on the Cross-Section of Laser Welded Joints

The different shapes of the cross section under 0–300 °C preheating temperature are shown in Figure 4. The profile of the cross section changed from funnel to X type when the preheating temperature increased from 0 to 300 °C. The top and bottom weld widths were larger than the middle width when the preheating temperature was over 150 °C. The top and bottom widths were plotted as a function of different preheating temperature shown in Figure 5. It can be concluded that when the preheating temperature increased to 300 °C, the bottom width increased from 0.77 to 2.75 mm, which was increased by 2.57 times compared to no preheating conditions. However, the top width increased only by 12.47% under preheating at 300 °C.

The increase of preheating temperature will increase the resistivity of the base metal, and the variation law is shown in Equation (2) [23].

$$\varrho = \varrho_{20}[1 + \gamma(T - 20)] \quad (2)$$

where ϱ_{20} is resistivity of metals at 20 °C (Ω·m); γ is temperature coefficient of resistance ($°C^{-1}$) and T is the temperature of preheating (°C).

The higher the resistivity of base metal, the lower the reflectivity of infrared ray. In the infrared band, the photon energy is low and can only be coupled with free electrons in the metal. The higher the metal resistivity, the greater the density of free electrons. The reflected wave generated by the forced vibration of free electrons is reduced, resulting in a decrease in reflectivity, which ultimately leads to an increase in laser absorption rate. The relationship between laser reflectivity and resistivity can be calculated with the Hagen–Rubens Equation (Equation (3)) [24].

$$R \approx 1 - 2/n \approx 1 - 2\sqrt{c\varrho/\lambda} \quad (3)$$

where R is laser reflectivity of metal and λ is laser wavelength (m).

Therefore, the increase of preheating temperature can effectively improve the laser absorption rate of base metals. The shape of cross section is only affected by the heat input, which means that the shape will not change with the same heat input [25]. When the same laser welding parameters are applied,

the higher the preheating temperature, the larger the weld width is. When appropriate preheating temperature is applied, higher penetration width can be obtained with lower welding parameters.

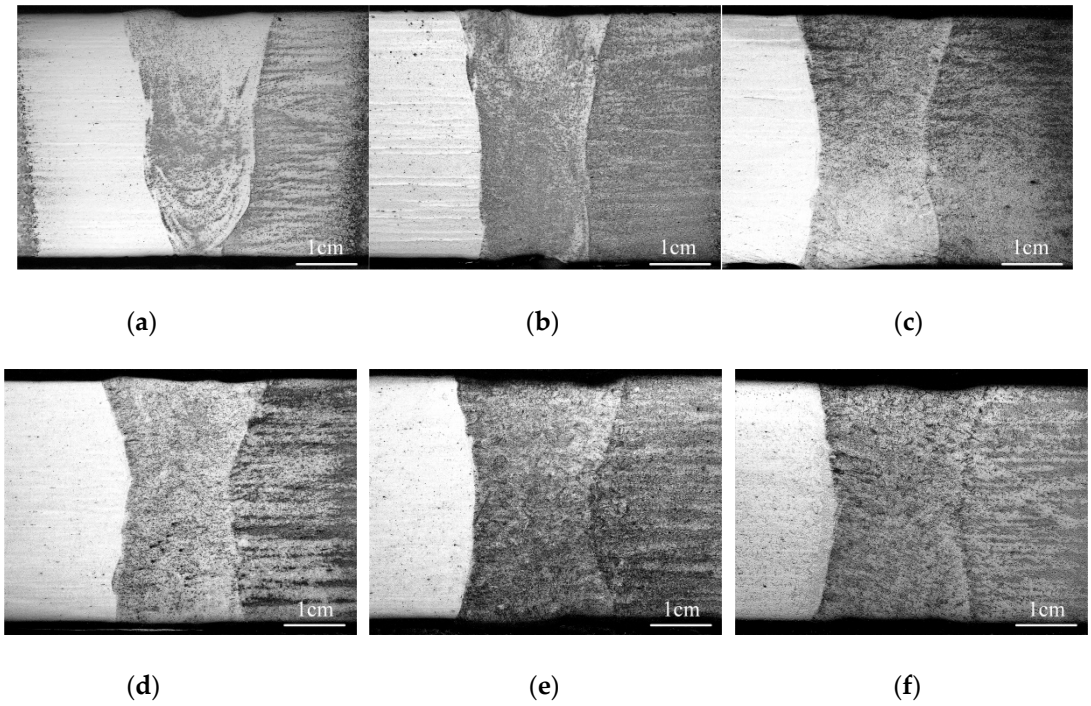

Figure 4. Effect of preheating on the cross-section of 42CrMo4/38MnVS6 laser welded joints: (**a**) without preheating; (**b**) 100 °C; (**c**) 150 °C; (**d**) 200 °C; (**e**) 250 °C; (**f**) 300 °C.

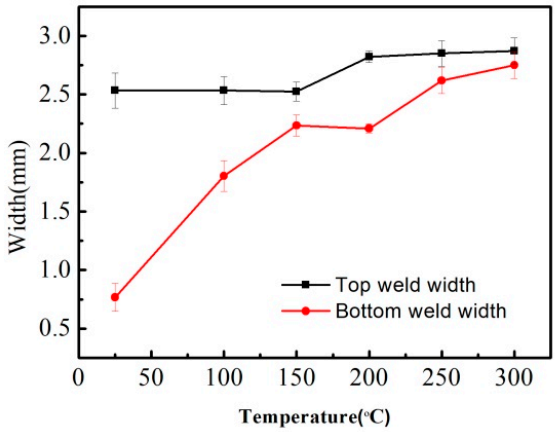

Figure 5. Effect of preheating on the weld width of 42CrMo4/38MnVS6 laser welded joints.

3.2. Effect of Preheating on Weld Microstructure

Figure 6 is the weld structure of laser welded joints without preheating and at preheating temperatures of 100 °C, 200 °C and 300 °C, respectively. The results show that the weld structure of laser welding without preheating and with preheating temperature of 100 °C is martensite. Bainite and acicular ferrite appear in the weld when the preheating temperature reaches 200 °C. When the preheating temperature reaches 300 °C, the volume of ferrite in the weld increases and becomes massive ferrite. The change of weld structure is related to the cooling rate after welding. The increase of preheating temperature decreases the cooling rate after welding. Bainite and ferrite structure begin to appear in the weld. There are differences in martensite structure in the weld zone of each joint. Figure 7 shows the XRD analysis of the weld zone at preheating temperature of 150 °C. There is no

obvious difference in phase composition of weld zone under different welding conditions, which is composed of martensite, Cr_7C_3, and $(Fe, Cr)_7C_3$.

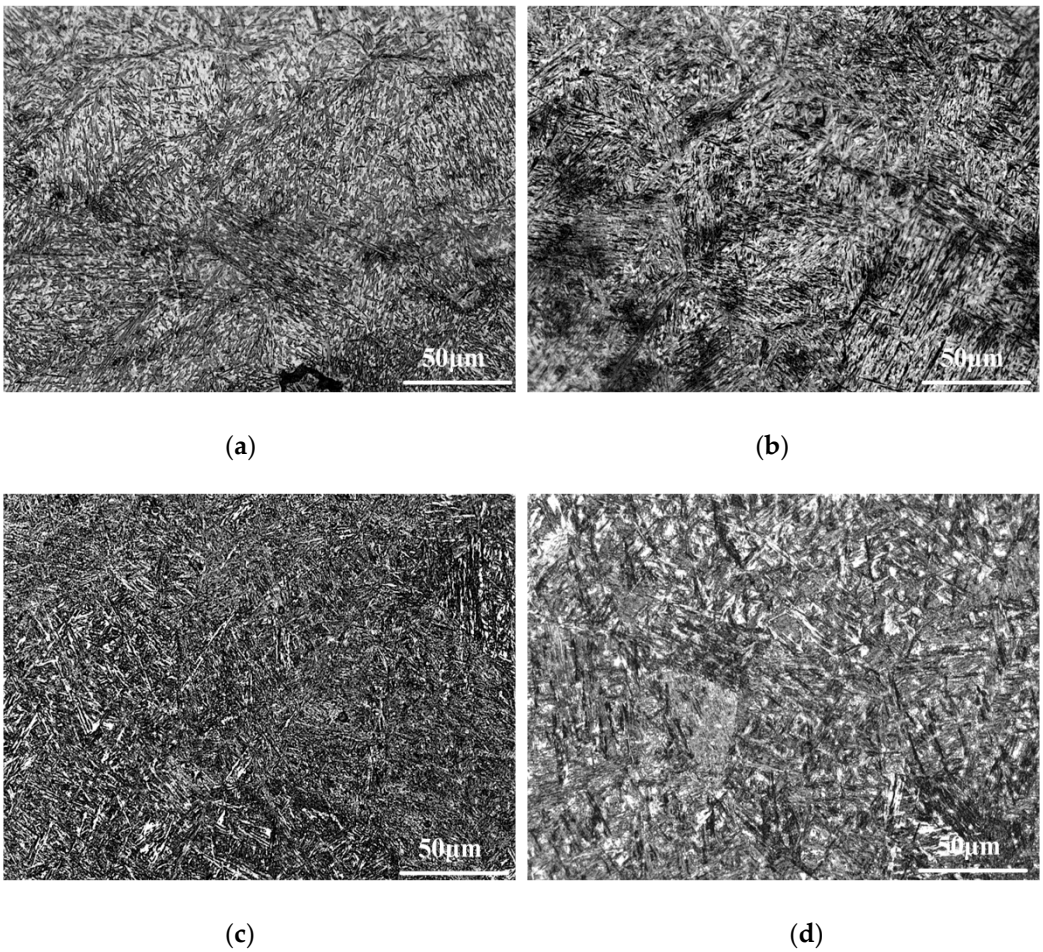

Figure 6. The structure of weld of 42CrMo4/38MnVS6 laser welded joint: (**a**) without preheat; (**b**) 100 °C; (**c**) 200 °C; (**d**) 300 °C.

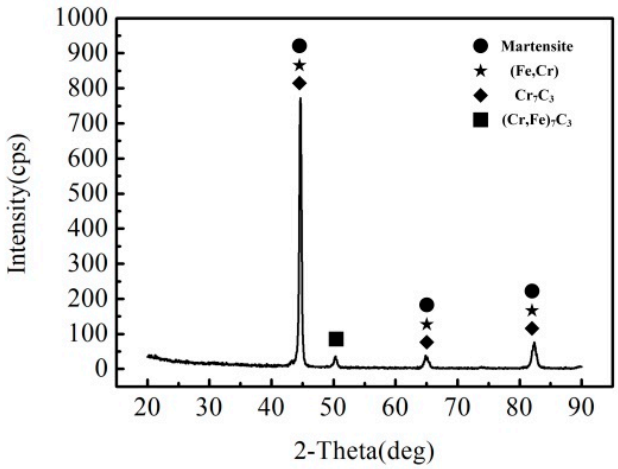

Figure 7. XRD of weld of 42CrMo4/38MnVS6 laser welded joint.

3.3. *Effect of Preheating on Martensite in Weld*

Figure 8 shows the martensite structure of the laser welded joint weld without preheating and preheating temperatures of 100 °C, 200 °C, and 300 °C. As the temperature of preheating increases

before welding, the morphology of martensite in the weld shows a tendency to change from twin martensite to lath martensite: Under the condition of no preheating, the microstructure of weld of laser welded joint is bamboo-shaped twin martensite. When the preheating temperature is 100 °C, the width of the twinned martensite sheet is reduced and distributed in bundles; when the preheating temperature is 200 °C, the martensite in the weld has a fine lath-like structure; when the preheating temperature reaches 300 °C, the lath martensite width is further increased, and the angle between the orientations is increased. A certain amount of $(Fe, Cr)_7C_3$ precipitates between the lath martensite.

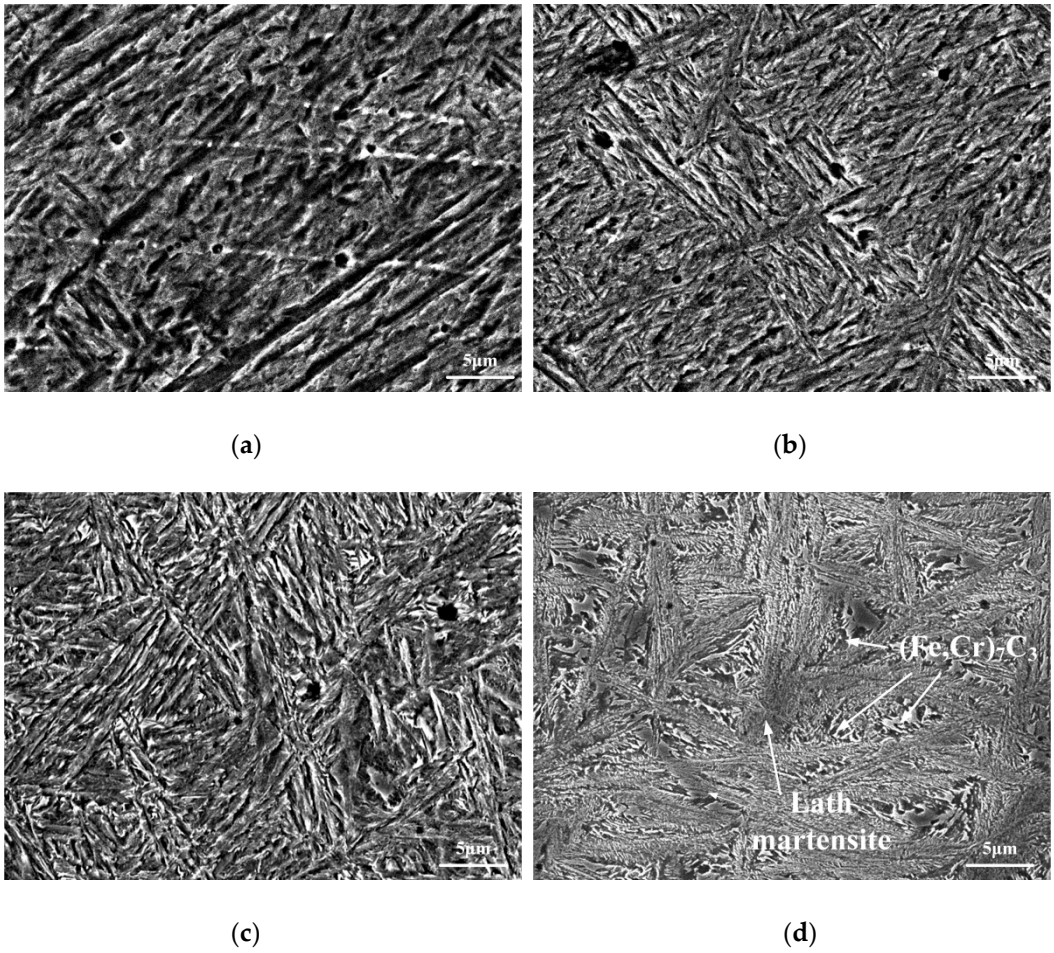

Figure 8. Martensite structure of weld zone of 42CrMo4/38MnVS6 laser welded joint: (**a**) single laser heat source; (**b**) 100 °C; (**c**) 200 °C; (**d**) 300 °C.

The weld of the 42CrMo/38MnVS6 laser welded joint is locally melted under the high temperature generated by the laser. During the cooling process, the liquid metal transforms into austenite, which is then converted into α-Fe and austenite, and finally the martensite structure is obtained. In this process, martensite nucleates and grows along the habitual surface in order to increase the volume by using the least interface energy. The high carbon content in the weld metal of 42CrMo/38MnVS6 laser welded joint leads to a larger interface energy, which can make the martensite fully grow up. Under the condition of laser heat source without preheating, large internal stress in the weld will increase the distortion energy, cause the increase of Ms (Martensite transformation starting temperature) and promote the formation of martensite when the cooling rate is high. Under the action of higher distortion energy, martensite begins to grow in the direction of mirror symmetry and twin structure is formed to adjust the distribution of strain energy in the weld.

With the increase of preheating temperature before welding, the ability of the base material to absorb laser light increases and the weld can obtain higher peak temperature and lower cooling speed under the action of the laser heat source of the same parameter. According to the Equation (4) [22]:

$$\begin{gathered} \Delta G^{\alpha \to M} = 2.1\sigma + 900 \text{ (J/mol)} \\ \sigma = 130 + 2800x + 0.2(800 - T) \text{ (MN/m}^2\text{)} \end{gathered} \quad (4)$$

where $\Delta G^{\alpha \to M}$ is the chemical free energy required for α-Fe to transform into martensite, σ is the yield strength of the matrix at Ms, x is carbon content, and T is temperature.

When the temperature is lowered, $\Delta G^{\alpha \to M}$ will increase, which will cause α-Fe to get sufficient driving force to transform into martensite. The increase of preheating temperature leads to the decrease of cooling rate after welding and the decrease of the temperature of M_S. When the T in Equation (4) is assigned to Ms, we can find from the formula that the decrease of Ms caused by the increase of preheating temperature will lead to an increase of the yield strength of the matrix and the driving force of martensitic transformation will increase. The decrease of Ms will cause the martensite transformation in the welds which are under preheating conditions to occur later than the weld under single laser heat without preheating. Therefore, austenite can stably enter the stage of α-Fe + γ, avoiding the high distortion energy caused by rapid volume change. Under the condition of low distortion energy and large driving force of martensite transformation, a large amount of martensite can continue to grow along the habitual surface, and a small amount of martensite can grow along the mirror symmetrical direction, so as to achieve the overall energy distribution balance and eventually form lath martensite, a large amount of martensite can continue to grow along the habit plane, and a small amount of martensite can grow along the mirror symmetrical direction, so as to achieve the balance of the overall energy distribution balance. The carbide which is $(Fe,Cr)_7C_3$ precipitate between lath martensite.

3.4. Effect of Preheating on Microhardness and Planar Fracture Toughness of Welds

The influence of preheating on the microhardness and plane fracture toughness of the weld is shown in Figure 9. The average microhardness of the weld metal without preheating is 820.9 HV. As the temperature of preheating increases, the microhardness of the weld gradually decreases. When the preheating temperature is 300 °C, the average microhardness of the weld metal is reduced to 433.6 HV; the plane fracture toughness (K1c) of the weld without preheating is 907.67 MPa·mm$^{-1/2}$. With the increase of heating temperature, the plane fracture toughness (K1c) shows a trend of rising and then decreasing: when the heating temperature is 150 °C, the plane fracture toughness (K1c) reaches the highest value of 2322.94 MPa·mm$^{-1/2}$. When the heating temperature is 300 °C, the plane fracture toughness (K1c) is 1427.08 MPa·mm$^{-1/2}$.

Figures 10 and 11 are the fracture morphologies of the weld seam in the plane fracture toughness test without preheating and at 150 °C, respectively. It can be seen from Figure 10 that there are pores in the weld seam of the laser welded joint without preheating; the fracture morphology at the loading force is rock sugar-like, showing obvious brittle fracture characteristics. It can be seen from Figure 8 that the dimple on the fracture at the weld at the preheating of 150 °C is a tear-extending dimple, exhibiting the characteristic of ductile fracture.

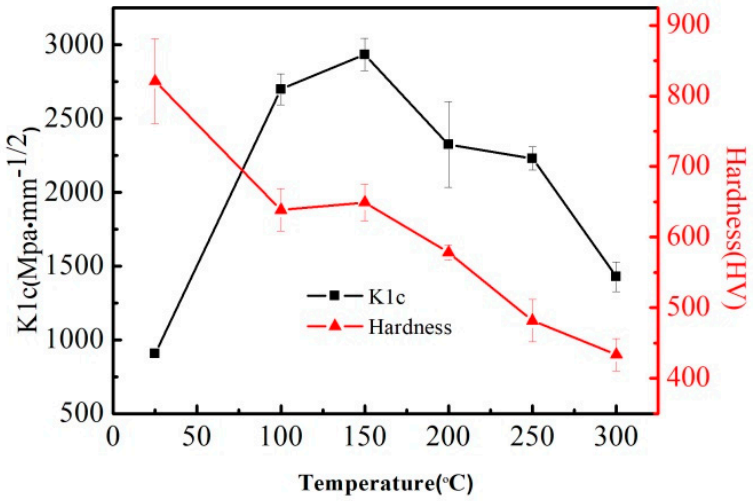

Figure 9. Effect of preheating on microhardness and plane fracture toughness of weld.

The microhardness of twin martensite in the weld without preheating is higher, which is due to the isotropy of martensite with disordered growth direction, the brittleness tends to be higher, and the fracture toughness is lower; With the increase of preheating temperature, the twin martensite in the weld begins to transform into lath martensite, and the martensite begins to change from isotropic to anisotropic, which causes crack propagation to be hindered and fracture toughness of weld improve. As the temperature of preheating continues to rise, the anisotropy of martensite begins to decrease, caused by the increase of the width of lath martensite, which accounts for the decrease of crack propagation's resistance, resulting in the decrease of the plane fracture toughness of weld finally.

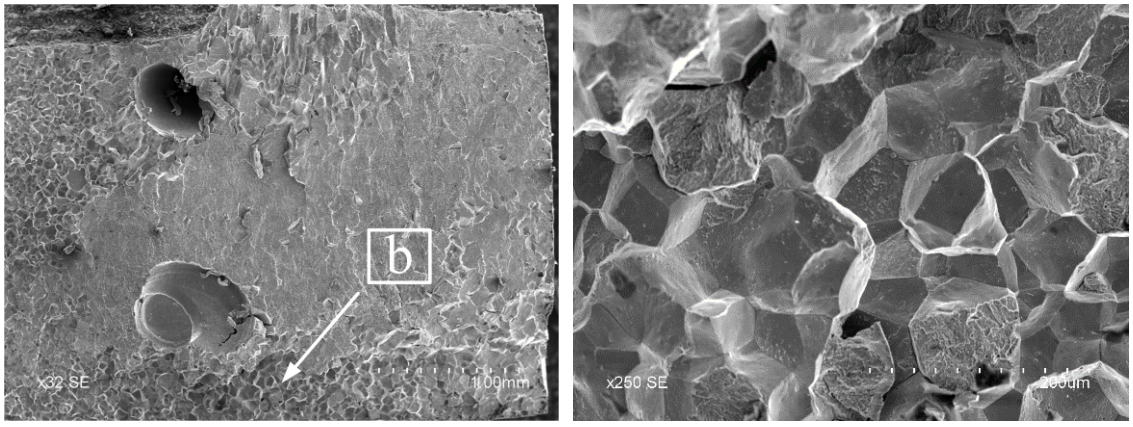

(**a**) (**b**)

Figure 10. The fracture of the weld without preheating in plane fracture toughness test: (**a**) The overall morphology; (**b**) the enlargement of b.

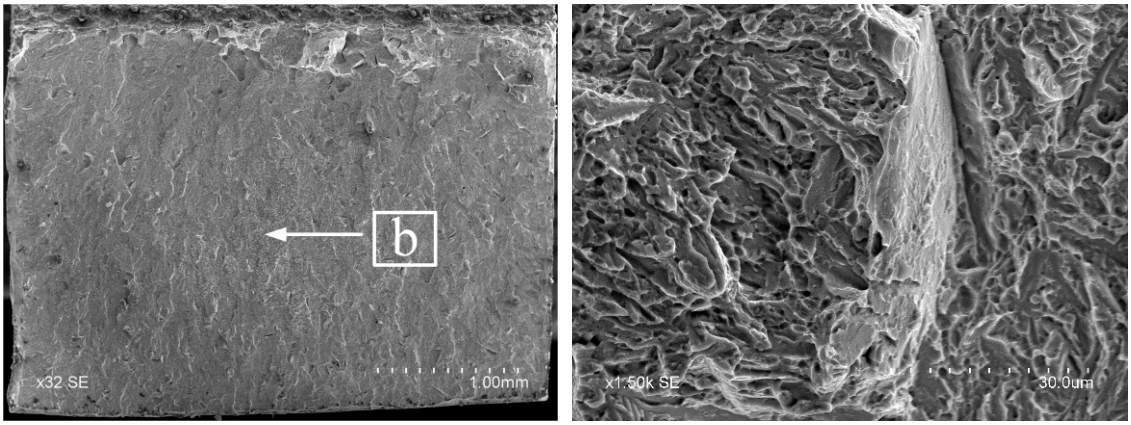

(**a**) (**b**)

Figure 11. The fracture of the weld with preheating at 150 °C in plane fracture toughness test: (**a**) The overall morphology; (**b**) the enlargement of b.

3.5. Effect of Preheating on Tensile Properties of Welded Joints

Figure 12 shows the effect of preheating on the tensile properties of welded joints. The tensile strength of the welded joint without preheating is low, and fracture occurs at the weld during tension; the tensile strength of the welded joint preheated before welding is improved. When the preheating temperature is 100–200 °C, the tensile strength of the welded joint is in the range of 1018.1–1032.5 MPa and the fracture occurred at the 38MnVS6 base metal; When the preheating temperature is from 250 °C to 300 °C, the tensile strength of the welded joint decreases. Figures 13 and 14 show the tensile fracture morphology without preheating and preheating at 150 °C, respectively. As shown in Figure 13b, the fracture surface without preheating exhibits predominant brittle fracture with flat cleavage planes. As illustrated in Figure 14b, the tensile fracture contains a large number of dimples and tear ridges and the fracture mode is ductile fracture.

The martensite of the weld microstructure without preheating is twining structure, with high microhardness and few slip systems. Under the condition of tensile stress, the toughness deformation of twin martensite is poor, which ultimately leads to brittle fracture at the weld; the martensite in the preheated weld before welding is mostly lath-like, with lower microhardness and more slip systems. Under the condition of tensile stress, ductile deformation can be carried out to improve the toughness of the welded joint. During the tensile process, the weld with higher toughness first reaches the three-direction stress state, and then the stress is transmitted to the base metal, which makes the fracture position occur in the base metal, and improves the tensile properties of the whole joint.

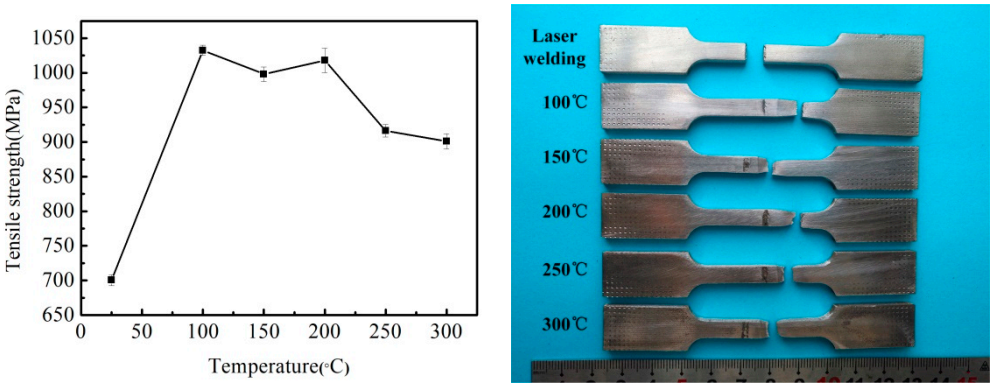

(**a**) (**b**)

Figure 12. Effect of preheating on tensile properties of 42CrMo/38MnVS6 laser welded joint: (**a**) effect of preheating temperature on tensile strength; (**b**) effect of preheating temperature on fracture location.

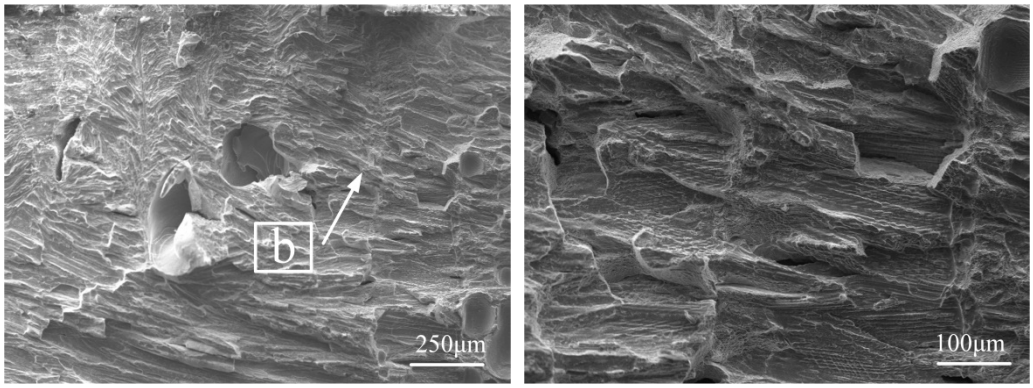

(**a**) (**b**)

Figure 13. The fracture of the welded joint without preheating in tensile test: (**a**) The overall morphology; (**b**) the enlargement of b.

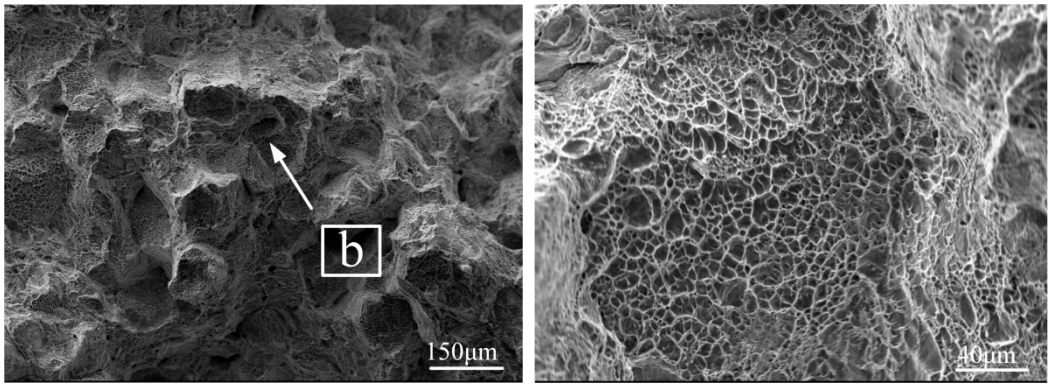

(**a**) (**b**)

Figure 14. The fracture of the welded joint with preheating at 150 °C in tensile test: (**a**) The overall morphology; (**b**) the enlargement of b.

4. Conclusions

The effects of different preheating temperatures on the microstructure and properties of 42CrMo/38MnVS6 laser welded joints were analyzed. The main results are summarized as follows:

i. The weld width of 42CrMo/38MnVS6 laser welded joint changes significantly with the preheating temperature increasing. As the preheating temperature changes from 0 to 300 °C, the weld joint varied from funnel type to X type with the bottom width increasing by 2.57 times. However, the top width increased only by 12.47%;

ii. The microstructure of weld without preheating is twin martensite with high hardness and poor toughness and the tensile fracture locates at the weld and belongs to brittle fracture;

iii. With the increase of preheating temperature before welding, the weld structure changes from twin martensite to mixed structure of lath martensite, ferrite and bainite, which is related to the change of distortion energy and strain energy. The increase of preheating temperature can reduce the distortion energy caused by volume change in weld and is beneficial to the growth of martensite along the habit plane, which promotes the formation of lath martensite;

iv. With the increase of preheating temperature, the average microhardness of the weld gradually decreases. The plane fracture toughness of the weld and the tensile strength of the welded joint first increase and then decrease. The mechanical properties of the welded joint are better when the preheating temperature is in the range of 100–200 °C.

Author Contributions: J.S. conducted microstructure analyses, microhardness test, analysis and interpretation of the results, and original draft preparation; X.Q. and Y.R. conducted methodology, editing, and visualization; F.X. and X.Q. conducted funding acquisition.

Funding: This research received no external funding.

Acknowledgments: The authors are grateful for the support of experimental works by Key Laboratory of Automobile Materials (Jilin University), Ministry of Education and Changchun Institute of Applied Chemistry Chinese Academy of Sciences.

Conflicts of Interest: The authors declare no conflict of interest.

References

1. Zeng, S.B. Development Trend of Piston Structure and Materials for Heavy Duty Diesel Engines. *Auto Manuf. Eng.* **2016**, *6*, 75–77.
2. Li, H.B.; Li, Y.J.; Wang, J. Research Status of Steel Piston Welding in Internal Combustion Engines. *Weld. Dig. Mach. Manuf.* **2018**, *1*, 20–25.
3. Gabriel, D.; Hettich, T. Top Weld(R) Steel Piston for High Speed Diesel Engine. *Foreign Intern. Combust. Engine* **2015**, *47*, 45–49.
4. Hisham, S.; Kadirgama, K.; Ramasamy, D.; Noor, M.M.; Amirruddin, A.K.; Najafi, G.; Rahman, M.M. Waste cooking oil blended with the engine oil for reduction of friction and wear on piston skirt. *Fuel* **2017**, *205*, 247–261. [CrossRef]
5. Du, S.J.; Gao, M.; Yan, X.B.; Zhang, Y.L. Friction welding parameters and joint microstructure analysis of forged steel pistons. *Welding* **2014**, *04*, 13–16.
6. Dong, H.; Yu, L.; Deng, D.; Zhou, W.; Dong, C. Direct Friction Welding of TiAl Alloy to 42CrMo Steel Rods. *Mater. Manuf. Process.* **2015**, *30*, 1104–1108. [CrossRef]
7. Wu, W. Study on Brazing Joint Process and Mechanism of TC4 Titanium Alloy and 38MnVS6 Steel. Master's Thesis, Harbin Institute of Technology, Harbin, China, 2017.
8. Datta, R.; Mukerjee, D.; Jha, S.; Narasimhan, K.; Veeraraghavan, R. Weldability characteristics of shielded metal arc welded high strength quenched and tempered plates. *J. Mater. Eng. Perform.* **2002**, *11*, 5–10. [CrossRef]
9. Yayla, P.; Kaluc, E.; Ural, K. Effects of welding processes on the mechanical properties of HY 80 steel weldments. *Mater. Des.* **2007**, *28*, 1898–1906. [CrossRef]
10. Chang, K.H.; Lee, C.H. Residual stresses and fracture mechanics analysis of a crack in welds of high strength steels. *Eng. Fract. Mech.* **2007**, *74*, 980–994. [CrossRef]
11. Naz, N.; Tariq, F.; Baloch, R.A. Failure analysis of HAZ cracking in low C–CrMoV steel weldment. *J. Fail. Anal. Prev.* **2009**, *9*, 370–379. [CrossRef]

12. Yoo, Y.T.; Ahn, D.G.; Ro, K.B.; Song, S.W.; Shin, H.J.; Im, K. Welding characteristics of S45C medium carbon steel in laser welding process using a high power CW Nd: YAG laser. *J. Mater. Sci.* **2004**, *39*, 6117–6119. [CrossRef]
13. Kuryntsev, S.V.; Gilmutdinov, A.K. Heat treatment of welded joints of steel 0.3C–1Cr–1Si produced by high-power fiber lasers. *Opt. Laser Technol.* **2015**, *74*, 125–131. [CrossRef]
14. Liu, W.J.; Shi, X.M.; Gao, B.; Ma, X.J. Development of a new type of laser welded integral forged steel structure piston. *Intern. Combust. Engine Power Plant* **2015**, *32*, 31–33.
15. Maurizi, M.; Hrdina, D. New MAHLE Steel Piston and Pin Coating System for Reduced TCO of CV Engines. *SAE Int. J. Commer. Veh.* **2017**, *9*, 270–275. [CrossRef]
16. Zhang, Y.; Chen, G.; Chen, B.; Wang, J.; Zhou, C. Experimental study of hot cracking at circular welding joints of 42CrMo steel. *Opt. Laser Technol.* **2017**, *97*, 327–334. [CrossRef]
17. Zhang, Y.; Chen, G.; Zhou, C.; Jiang, Y.; Zhong, P.; Li, S. Pores formation in laser–MAG welding of 42CrMo steel. *J. Mater. Process. Technol.* **2017**, *245*, 309–317. [CrossRef]
18. Köse, C.; Kaçar, R. The effect of preheat & post weld heat treatment on the laser weldability of AISI 420 martensitic stainless steel. *Mater. Des.* **2014**, *64*, 221–226.
19. Hu, L.H.; Huang, J.; Li, Z.G.; Wu, Y.X. Effects of preheating temperature on cold cracks, microstructures and proper- ties of high power laser hybrid welded 10Ni3CrMoV steel. *Mater. Des.* **2011**, *32*, 1931–1939. [CrossRef]
20. Piekarska, W.; Goszczyńska-Króliszewska, D.; Domański, T.; Bokota, A. Analytical and Numerical Model of Laser Welding Phenomena with the Initial Preheating. *Procedia Eng.* **2017**, *177*, 149–154. [CrossRef]
21. Yan, L.; Xinhua, T.; Haichao, C.; Hailiang, X.; Zhipeng, R.; Houyin, Y. Effect of Preheating Temperature on the Microstructure of QSTE420TM+X C45 Dissimilar Steel Laser Welded Joints. *Rare Met. Mater. Eng.* **2013**, *42*, 50–54.
22. Song, M.X.; Wang, H.; Liu, Z.H.; Sun, B. Effect of preheating on laser weld formation of aluminum alloy. *Welding* **2018**, *02*, 51–53, 64.
23. Liu, Q.B. *Laser Processing Technology and Its Application*; Metallurgical Industry Press: Beijing, China, 2007.
24. Sun, C.W.; Lu, Q.S.; Fan, Z.X.; Li, C.F. *Laser Irradiation Effects*; National Defense Industry Press: Beijing, China, 2002.
25. Lu, F.; Li, X.; Li, Z.; Tang, X.; Cui, H. Formation and influence mechanism of keyhole-induced porosity in deep-penetration laser welding based on 3D transient modeling. *Int. J. Heat Mass Transf.* **2015**, *90*, 1143–1152. [CrossRef]

© 2019 by the authors. Licensee MDPI, Basel, Switzerland. This article is an open access article distributed under the terms and conditions of the Creative Commons Attribution (CC BY) license (http://creativecommons.org/licenses/by/4.0/).